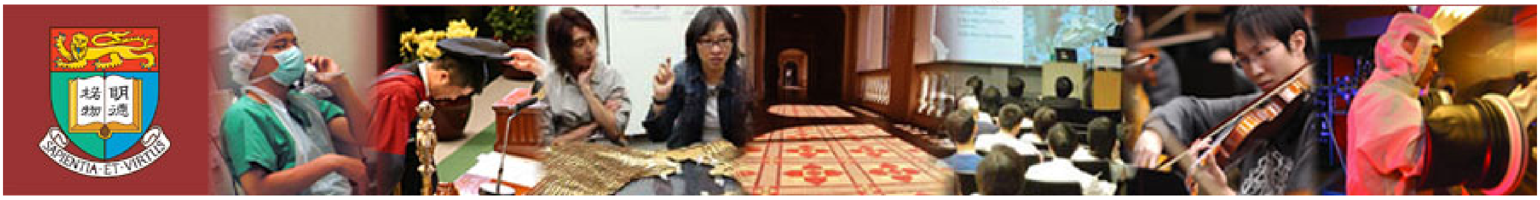

Title	Single mode operation of impurity-induced disordering large area vertical cavity surface emitting lasers
Author(s)	Lo, CW; Yu, SF
Citation	Infrared applications of semiconductors: materials, processing and devices, Materials Research Society Symposium Proceedings, Boston, Massachusetts, 2-5 December 1996, v. 450, p. 147-152
Issued Date	1997
URL	http://hdl.handle.net/10722/46029
Rights	Materials Research Society Symposium Proceedings. Copyright © Materials Research Society.

SINGLE MODE OPERATION OF IMPURITY-INDUCED DISORDERING LARGE AREA VERTICAL CAVITY SURFACE EMITTING LASERS

C.W. Lo and S.F. Yu
The University of Hong Kong, Department of Electrical and Electronic Engineering, Pokfulam Road, Hong Kong.

ABSTRACT

Vertical-cavity surface-emitting lasers (VCSELs) with suitable interdiffusion quantum wells profile by the use of selective impurity-induced disordering is proposed for high power single mode operation in large area devices. It is shown that the transverse optical confinement in the quantum well active region formed by the diffusion profile counteracts the influence of carrier spatial hole burning for VCSELs biased at high injection current. Results indicate that a single mode operation can be maintained in VCSELs with the diameter of core region equal to 50μm.

INTRODUCTION

VCSELs are becoming one of the promising devices for various applications in high bit-rate optical fiber communication system, optical parallel processing and optical interconnections. This is because of their unique features such as small circular output beam divergence, single longitudinal mode operation with low threshold currents less than 1mA and high relaxation oscillation frequency [1-3]. However, the excitation of higher order transverse modes degrades VCSELs' performance in high speed optical communication systems and should be avoided. To achieve the above applications, a single fundamental transverse mode operation is essential due to the elimination of noise and instability and the ease of higher coupling efficiency with optical fibers [4]. In index guided VCSELs, the number of modes depends on their transverse dimensions and the refractive index profile between the core and cladding regions. In gain guided VCSELs, the fundamental transverse mode operation can be maintained for large area devices. However, higher order transverse modes are excited with high injection currents due to spatial hole burning effect within the core region [5]. Therefore, it is necessary to suppress the multiple transverse modes in VCSELs at high output power for large area devices.

Concentration of impurity varies the refractive index and carrier diffusion rate of diffused quantum well (DFQW) material [6]. A defined pattern of refractive index profile can be obtained by selective area disordering of quantum well materials and this technique can be utilized for the fabrication of optical devices such as lasers and modulators [7]. In this paper, single mode operation of large area VCSELs using selective disordering of quantum well active region is studied theoretically.

LASER STRUCTURE

The schematic of VCSEL after selective impurity-induced disordering is shown in figure 1. It is assumed that the active layer consists of 20 $Al_{0.3}Ga_{0.7}As$/GaAs quantum wells with well width and barrier thickness of 100Å and 100Å, respectively. In order to achieve a single mode operation of VCSELs, the transverse optical confinement in the quantum well active region is produced by the use of selective impurity-induced disordering technique. The selective injection of impurities can be done by using a circular mask located at the center of the core region to

Mat. Res. Soc. Symp. Proc. Vol. 450 © 1997 Materials Research Society

shelter from the ion implantation. A suitable distribution of impurity along the transverse direction of impurity can be obtained with appropriated annealing time and temperature. Therefore, dimension of mask, implantation energy, annealing temperature and time are the parameters to optimized the gain margin of VCSELs.

LASER MODEL

The multimode rate equation model of VCSEL used in our analysis are given as follows [8]

$$\frac{\partial N(r,t)}{\partial t}=\frac{J(r,t)}{qd_k}-\frac{N(r,t)}{\tau}+D\frac{1}{r}\frac{\partial}{\partial r}\left(r\frac{\partial N(r,t)}{\partial r}\right)-v_g\Gamma_z G(r,t)\sum_i |E_i(r)|^2 S_i(t) \tag{1}$$

$$\frac{\partial S_i(t)}{\partial t}=v_g(\Gamma_z G_i-\alpha_i)S_i(t)+R_{sp}(t) \tag{2}$$

where N is the transverse distribution in the radial direction, r of carrier concentration inside the active layer and S_i is photon density of the ith mode. d_k is the thickness of the active layer, q is the electron charge, τ is the carrier lifetime, Γ_z is the longitudinal confinement factor, v_g (=c/n_g, where n_g is the group index and c is the velocity of light in free space) is the group velocity and D is the ambipolar diffusion coefficient. α_i is the scattering loss in the active layer for ith mode and Rsp is the spontaneous emission rate. J(r, t) is the current density distribution along the transverse direction.

In the photon rate equation, the effective optical gain G_i of the ith mode is given by

$$G_i=\frac{2}{w^2}\int_0^\infty g(N)|E_i(r,t)|^2\, r\,dr\,, \tag{3}$$

where g is the optical gain of the quantum well's active layer to be determined.

The symbol E_i represents the normalized slowly varying complex field intensity (i.e. $1=2\int_0^\infty |E_i|^2\, r dr/w^2$) for the ith mode with S_i as the corresponding photon density. The field intensity ,E_i, can be determined by solving the complex scalar Helmholtz equation. It is expected that the active layer supports the transverse modes which can be expressed in terms of linearly-polarized ($LP_{\ell p}$) modes where the indexes ℓ and p denote the azimuthal and radial order of modes respectively. The LP_{01} mode is dominated due to its maximized overlapping with the optical gain profile, however, the LP_{11} mode can also be excited for the reasons of non-uniform current injection and spatial hole burning effects. Therefore, the influence of modes competition (between LP_{01} and LP_{11} modes) is also taken into calculation. The subscript i=1 and i=2 of the above equations represent the case of LP_{01} and LP_{11} mode respectively.

The threshold and above threshold behavior of VCSELs with selective disordering is obtained from equation (1) and (2) by setting the time-derivatives equal to zero. These non-linear and time independent simultaneous rate equations can be solved in a self-consistent manner. The lateral variation along carrier concentration of the active layer is also solved by using finite difference method subject to the condition that N and its derivative are continuous everywhere. If we assume the circular symmetry of carrier concentration, at r=0, the first and second derivative of N take the form as follow :

$$\left.\frac{\partial N}{\partial r}\right|_{r_1}=0\,, \tag{4}$$

$$\left.\frac{\partial^2 N}{\partial r^2}\right|_{r_1}=\frac{2\left(N(r_2,t)-N(r_1,t)\right)}{\Delta r^2} \tag{5}$$

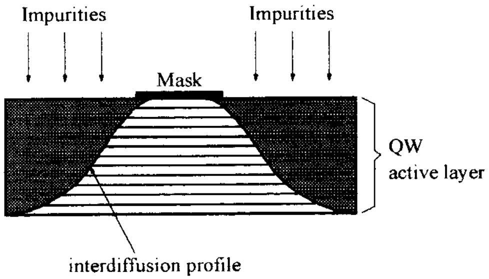

Figure 1. Schematic of a VCSEL after selective disordering

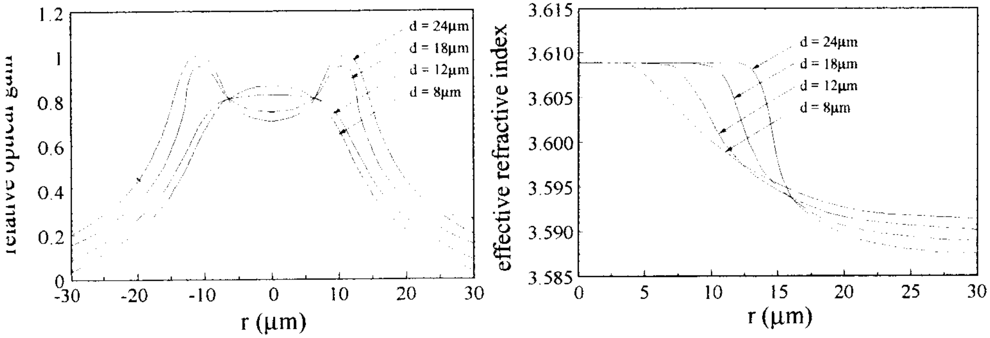

Figure 2. The optical gain and refractive index distribution of VCSEL with the diameter of mask, d varied between 8 to 24 μm.

where Δr is the separation between two successive points in the radial direction, r. It is also required that as r → very large, the carrier concentration change N → 0. The field intensity E_i is also solved simultaneously with the carrier concentration such that the time-dependent transverse field intensity variation can also be considered into investigation.

MODEL FOR QUANTUM WELL MATERIAL

The refractive index and optical gain of quantum wells material under the influence of impurities induced disordering are also considered in our analysis. The models given in references [9,10,11] are utilized to calculate the optical and electrical properties of DFQW's which are summarized in Appendix A. It is defined that the extent of interdiffusion into the quantum wells material is characterized by a diffusion length, L_d, where L_d=0Å represents the as-grown quantum wells and the diffusion strength of impurity is described by the magnitude of L_d. The corresponding magnitude of L_d between the mask and non-mask region are equal to 0 and 10Å, respectively. In the following calculation, the values of DFQW's parameters vary with L_d and device parameters used in the laser model are given in Table I and II, respectively.

Table I. Material Parameters in Laser Structure

(at operating wavelength of 0.85μm)	Diffusion Length (L_d)	
	0 Å	10 Å
Fitted parameters (a_N) cm^{-1}	1780.0121	468.6990
Transparency carrier density (N_o)x$10^{18}cm^{-3}$	2.1996	2.4092
Fitted parameters (e)	-0.02824	-0.02521
Fitted parameters (N_r)x$10^{18}cm^{-3}$	2.0673	1.9809
Refractive index (n_β)	3.627	3.5880

Table II. Parameters Used in Model

Parameters (symbol)	Magnitude
Thickness of active region (d)	1 μm
Carrier lifetime (τ)	4 ns
Effective group refractive index (n_g)	3.70
Longitudinal confinement factor (Γ_z)	0.16
Velocity of light in free space (c)	$3x10^{10}$ cms^{-1}
Ambipolar diffusion coefficient (D)	15 cm^2s^{-1}

RESULTS & DISCUSSIONS

It is assumed that the laser is initially biased at threshold and modulated by a step current of 2 times its threshold value. The operating wavelength of the VCSEL is chosen to be λ_o = 0.85μm and the diameter of core region is equal to 50μm. The diameter of circular mask, d is varied between 8 and 24μm to shelter from the ion implantation. In order to ensure the current is effectively injected in the laser, the current confinement structure is needed. It is observed that the relative optical gain at the center of core region of DFQW-VCSEL is suppressed for the increasing diameter of circular mask. With the cases of the diameter of circular mask equal to 8μm and 12μm, the transverse optical confinement in the quantum well active region is produced. This is because a gaussian distribution of permittivity along the active layer is produced by the impurities andthe transverse field is guided. The gain margin can also be enhanced if the overlapping integral between the optical gain and the fundamental transverse mode is maximized.

Figure 3 shows the near field profile of DFQW-VCSEL with the diameter of circular mask varied between 8 and 24μm. It is found that the fundamental mode of optical field can not be maintained for large size of circular mask. This is because the active layer of DFQW-VCSEL with large circular mask no longer supports the LP_{01} transverse mode. Moreover, the excitation of higher-order transverse mode is observed due to the spatial hole burning effects. Therefore, the dimension of the circular mask can affect the performance of DFQW-VCSEL.

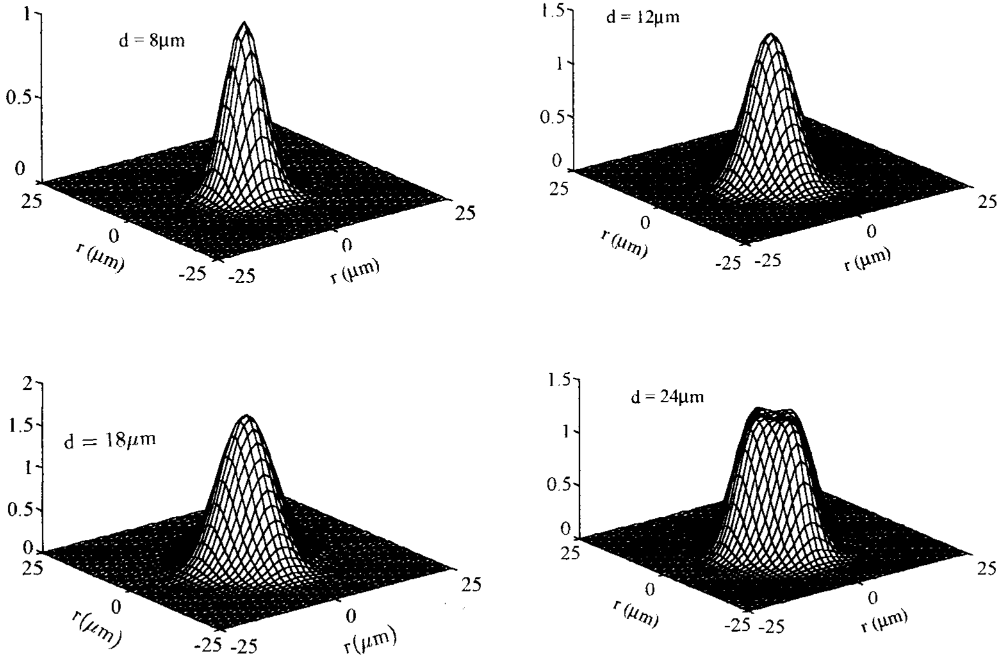

Figure 3. The near field profile with the diameter of mask, d, varied between 8 to 24 μm.

CONCULSION

In conclusion, the selective impurity-induced disordering vertical-cavity surface-emitting lasers with the diameter of the core region equal to 50μm is investigated. These devices are designed to achieve a high power single mode opearion at 0.85μm. Results show that the single mode operation with the diameters of the circular mask varied between 8 and 18μm are obtained. The confinement of the transverse optical field is produced by using selective IID technique can reduce the influence of the carrier spatial hole burning at high injection current. Therefore, the behaviour of the DFQW-VCSEL is affected by the size of the circular mask. Besides, the implanation energy, annealing temperature and time are also the important parameters to determine the modal behaviour of DFQW-VCSEL.

APPENDIX A

The refractive index, n_{DFQW}, of diffused quantum wells active layer is given by [9]

$$n_{DFQW}(\omega) = \left(\tfrac{1}{2}\varepsilon_1^{\Gamma}(\omega) + \tfrac{1}{2}\left\{ \left[\varepsilon_1^{\Gamma}(\omega)\right]^2 + \left[\varepsilon_2^{\Gamma}(\omega)\right]^2 \right\}^{1/2} \right)^{1/2} \qquad \text{(A1)}$$

where ω is the angular frequency, $\varepsilon_1^{\Gamma}(\omega)$ and $\varepsilon_2^{\Gamma}(\omega)$ are the real and imaginary parts of the total dielectric function for the Γ valley, respectively.

Using density matrix approach, the optical gain with photon generated in the direction perpendicular to the surface of quantum well layers is given as [11]

$$g(\omega)=\frac{e^2M_b^2}{\pi c\varepsilon m_o^2\omega L_z}\sum_{p,q}\int\left|\left\langle\psi_{Cp}|\psi_{Vq}\right\rangle\right|^2\mathbf{P}_{pq}(k)$$
$$\times\mathbf{L}\left[E_p(k)-E_q(k)-\eta\omega\right]\left\{f^C\left[E_p(k)\right]-f^V\left[E_q(k)\right]\right\}dk \tag{A2}$$

where m_0 is the rest mass of electron and M_b is the optical matrix. E_p and E_q are the pth-electron and qth-hole sub-band-edge energy, respectively, ψ_C and ψ_V are the envelope wavefunctions for the electrons and holes, respectively. **L** is the Lorentzian broadening factor with HWHM of 5meV and k is the wavevector. The summation in (A2) is over all the conduction and valence sub-bands and **P**(k) is the TE-polarization factor. f^C and f^V are the quasi-Fermi for the electrons in the conduction and valance bands, respectively.

It is noted from our calculation that at a particular L_d and at an external carrier injection level, N, the TE net optical gain spectrum at room temperature is found to have a simple expression, $g(\omega)=a_N\ln(N/N_0)$, where a_N is the fitted parameter and N_0 is the carrier concentration at transparency. The parameters a_N and N_0 at particular frequency vary with L_d are given in Table I.

The carrier induces refractive index change, Δn, which varies with the background refractive index profile of active region, can be obtained from the change of gain coefficient, $\Delta g(\omega)=g(\omega)-g_0(\omega)$, through the Kramers-Kronig dispersion relation [10]

$$\Delta n(\omega)=\frac{\pi}{c}PV\int_0^\infty\frac{\Delta G(\omega')}{\omega'^2-\omega^2}d\omega' \tag{A3}$$

where $g_0(\omega)$ is the optical gain at transparency. The symbol PV stands for the Cauchy principle value. We can also show that at a particular L_d the relation between Δn and N can be expressed as, $\Delta n=e\ln(N/N_r)$, where e and N_r are fitted parameters vary with L_d and also given in Table II.

REFERENCES

[1] Y. H. Lee, B. Tell, K. Brown-Goebeler, J. L. Jewell and J. V. Hove, Electron. Lett., **26**, 710 (1990).

[2] R. S. Geels and L. A. Coldren, Appl. Phys. Lett., **57**, 1605 (1990).

[3] D. Tauber, G. Wang, R. S. Geels, J. E. Bowers, and L. A. Coldern, Appl. Phys. Lett., **62**, 325 (1993).

[4] C. J. Chang-Hasnain, M. Orenstein, A. Von Lehmen, L. T. Florez, J. P. Harbison and N.G. Stoffel, Appl. Phys. Lett., **57**, 218 (1990).

[5] A. Valle, J. Sarma and K. A. Shore, IEEE J. Quantum Electron., **31**, 1423 (1995).

[6] E. H. Li and B. L. Weiss, IEEE J. Quantum Electron., **29**, 311 (1993).

[7] R. P. Bryan, J. J. Coleman, L. M. Miller, M. E. Givens, R. S. Averback and J. L. Klatt, Appl. Phys. Lett., **55**, 94 (1989).

[8] G. Ronald Hadley, K. L. Lear, M. E. Warren, K. D. Choquette, J. W. Scott and S. W. Corzine, IEEE J. Quantum Electron., **32**, 607 (1996).

[9] E.H. Li, B.L. Weiss, K.S. Chan and J. Micallef, Appl. Phys. Lett. **62** , 550, (1992).

[10] C.H. Herny, R.A. Logan and K.A. Bertness, J. Appl. Phys. **52**, 4457, (1981).

[11] E.H. Li and K.S. Chan, Electron. Lett., **29**, 1233, (1993).